Surface structure and bonding in the strongly correlated metal oxides NiO and UO_2

M. R. Castell,[a] S. L. Dudarev, C. Muggelberg, A. P. Sutton, and G. A. D. Briggs
Department of Materials, University of Oxford, Parks Road, Oxford OX1 3PH, United Kingdom

D. T. Goddard
Research and Technology, BNFL, Springfields Works, Salwick, Preston, Lancashire PR4 OXJ, United Kingdom

(Received 28 October 1997; accepted 24 November 1997)

We show atomic resolution elevated temperature scanning tunneling microscope images of the NiO (001) and UO_2 (111) surfaces. When imaging the empty states structure of NiO, a fourfold symmetric hole state is observed around defects and step edges which influences the second nearest neighbor Ni ions. A similar effect is not observed on the UO_2 (111) surface. We explain this difference in terms of the degree of covalent coupling that is involved in the bonding of these oxides. Modeling of the electronic structure through the local spin density approximation incorporating the Hubbard U is used to create charge density maps which show that there is a significant element of nonsphericity of charge distribution around the Ni ions in NiO, but that the distribution is spherical in UO_2. © *1998 American Vacuum Society*. [S0734-2101(98)00403-5]

I. INTRODUCTION

Surface studies of metal oxides are of crucial importance in a diverse range of fields in chemistry and materials science including catalysis, gas sensing, and corrosion studies.[1] While metal oxides can be conductors or semiconductors, many are insulators at room temperature due to their wide band gaps. This limits the range of surface science techniques that can be used to study their properties, and means that scanning tunneling microscopy (STM) can only be carried out at elevated temperatures where the conductivity is sufficiently high. We have investigated two metal oxides, UO_2 and NiO, whose room temperature resistivity is too high to allow successful STM imaging, but which can be imaged with atomic resolution at elevated temperatures.

While NiO and UO_2 should undoubtedly be placed into the class of wide band gap ionic room temperature insulators, there are a number of issues concerning both the origin of their band structure and the ionicity of these materials that demand serious attention. In the purely ionic scheme the metal cations have a partially filled valence shell which, according to conventional band theory based on the local spin density approximation (LSDA), should result in metallic behavior. In fact the study of transition and actinide oxides reveals that the electronic structure of many compounds is dominated by the presence of strong on-site Coulomb repulsion (strong correlations) between valence electrons localized on metal ions. This means that in order to perform successful modeling of the electronic structure it is necessary to include correlation effects in an *ab initio* computational scheme. A local spin density approximation approach has been developed that includes the Hubbard U term describing the electron interactions (LSDA+U).[2–5] This allows accurate modeling of the electronic structure of UO_2 and NiO, which in turn is required for STM image interpretation. By combining the evidence from STM and LSDA+U we show that there is a significant covalent element to bonding in NiO, whereas UO_2 is almost entirely ionic.

II. EXPERIMENTAL PROCEDURES

The UO_2 (111) surfaces were prepared by cutting and polishing and were subsequently reacted with HF(g) to form a UF_4 layer.[6] This layer was removed in 0.2 M HNO_3, rinsed, and the sample was immediately introduced into the UHV chamber of the STM. The (111) surface was then cleaned by annealing in UHV ($\sim 10^{-8}$ Pa) at 760 °C for 8 h. NiO crystals doped with 0.5% Li were cleaved under UHV revealing a (001) surface, with no further treatment being required.

The STM experiments on UO_2 were carried out in a JEOL JSTM-4500XT elevated temperature STM at 400–500 °C using etched Pt/Ir tips. Imaging of NiO crystals was performed at 200 °C with etched W tips. Low energy electron diffraction (LEED) and Auger electron spectroscopy were used to determine the condition of the surface prior to STM investigation. The STM images presented in this article were all from clean, well-ordered surfaces.

III. STM OF NiO (001)

NiO cryzsallizes into the simple rocksalt structure and cleaves extremely well on (001) planes. The typical mesoscopic topography that is generated by cleavage consists of (001) terraces up to 50 nm wide which are predominantly separated by monatomic steps that run in ⟨001⟩ directions.[7] The terraces generally have a low defect density and are arranged in the bulk terminated (1×1) structure as shown in an empty states STM image in Fig. 1(a). LSDA+U modeling of the states that extend into the vacuum shows that the lower edge of the conduction band is predominantly due to

---

[a] Electronic mail: martin.castell@materials.ox.ac.uk

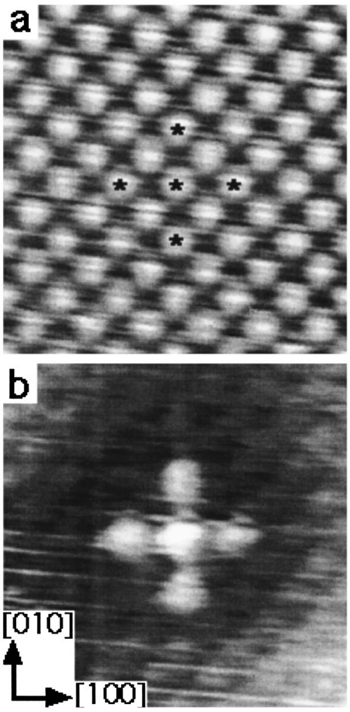

FIG. 1. Empty states STM images of the NiO (001) surface. In (a) the (1×1) lattice reveals only the Ni sites and not the O sites although they are both present on the same surface plane. An image of a typical point defect on the Ni sublattice (b) shows how a single atom perturbation causes the four second nearest neighbor Ni sites to brighten. The equivalent positions of the bright Ni sites in (b) are indicated by stars on the image in (a). Image width 2.5 nm, sample bias 1.1 V (a) and 1.2 V (b), tunneling current 1 nA.

Ni states, and as oxygen and nickel ions are located in the same surface plane, it is most likely that the atomic structure in Fig. 1 reveals the Ni sites. Filled-states images of the surface show the (1×1) oxygen lattice, though the corrugation height is much smaller in this case.[5,7] The full experimental details and further results of STM imaging of the NiO (001) cleavage surface are described elsewhere.[5,7,8]

What we will concentrate on here is the second nearest neighbor (SNN) brightening in empty states STM images around single atom Ni sublattice defects as shown in Fig. 1(b). This image shows a delocalized gap state that is created when there is a perturbation on the Ni sublattice. In Fig. 1(b) the center of the defect lies on the Ni sublattice with the four SNN Ni sites also appearing bright. This cross of five highlighted Ni sites is the smallest unit in which this type of defect appears. We interpret the cross structure as a single atom perturbation on the Ni sublattice, which could either be a Ni vacancy or a substitutional atom (e.g., Li or Fe). The four SNN Ni sites are highlighted because a delocalized gap state is created by the perturbation that extends over the defect and the four SNN Ni ions. In fact the defect state almost certainly extends further than the four SNN Ni ions, but is too weak to be imaged. The empty states STM image of Fig. 1(b) displays a ''large-scale'' manifestation of directional coupling between SNN Ni ions which is analogous to stating that effects of covalent bonding can be observed in the STM image. In a sense the extension of this statement to covalent bonding is a little misleading because in Fig. 1(b) we are looking at empty states STM images, so in the ground state of NiO there would not be any electrons in this state to contribute to the actual covalent bonding. However, the important observation is that there is strong SNN Ni *d* symmetry coupling via an intermediate O ion which cannot be explained using a purely ionic model.

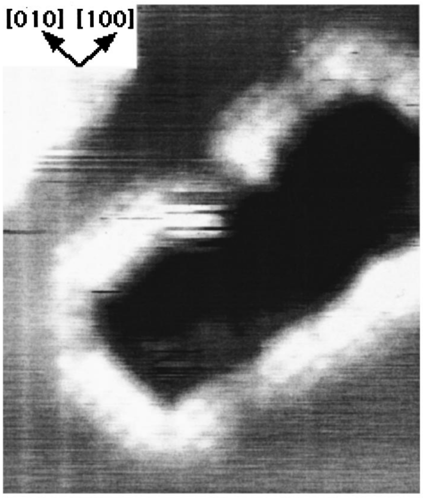

FIG. 2. Empty states STM image (9 nm image width) of terraces separated by a monatomic step taken at a sample bias of +0.7 V and with a 1.0 nA tunneling current. This image shows the presence of extended $c(2\times2)$ patterning which only occurs above $\langle 001\rangle$ step edges.

Extended patterning of the same nature as shown in Fig. 1(b) can be observed above $\langle 001\rangle$ step edges[7,8] as shown in Fig. 2. This patterning occurs because every Ni ion in the second row inwards from the top of a $\langle 001\rangle$ step edge is coordinated in the same way as the SNN Ni ions were around the Ni defect site. The step edge essentially acts as a row of Ni vacancies resulting in extended patterning above the step edge.

IV. STM OF UO_2 (111)

Previous STM studies of UO_2 (111) have shown that this surface is very similar to a simple termination of the bulk fluorite lattice.[9,10] This result agrees with other studies including LEED, Rutherford backscattering, and ion scattering spectroscopy.[6,11–13] A typical STM image of the (111) surface is shown in Fig. 3. The underlying three-fold symmetry of the (111) surface can be seen with 3.9 Å periodicity along the $\langle 110\rangle$ directions. It is not possible to determine from the STM image alone whether uranium or oxygen atoms are being imaged. The (111) surface has an oxygen termination as the top-most layer, but between each oxygen atom, and 0.7 Å further into the bulk, there are uranium atoms with the same (1×1) lattice periodicity. Due to the dominance of the

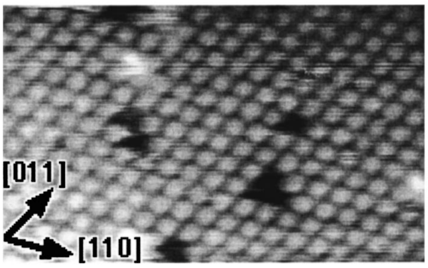

FIG. 3. Empty states STM image of the UO_2 (111) surface. The (1×1) lattice periodicity is most likely due to uranium sites. Missing uranium ions do not create an observable perturbation on their neighbors. Image width 8.4 nm, sample bias 1.9 V, tunneling current 0.7 nA.

uranium density of states (DOS) at the bottom of the conduction band it is likely that the uranium sites are imaged at positive sample bias.[4] This conclusion is based on the analysis of the bulk electronic structure, while the STM probes the electronic structure in the surface region. In order to confirm that the bright lattice positions in Fig. 3 correspond to uranium sites, it will be necessary to calculate the corresponding surface electronic structure.

A further argument that supports that the uranium sites are being imaged is that a number of point vacancies can be observed. The UO_2 crystals are slightly overstoichiometric with the additional oxygen incorporated in interstitial positions. This interstitial oxygen is highly mobile at the imaging temperature (~500 °C) and is likely to have filled the defects in Fig. 3 if they were oxygen vacancies—clearly this is not the case.

A significant observation in Fig. 3 is that the point defects in the image simply appear as vacancies without causing a detectable brightening or darkening of the surrounding uranium sites. This observation is true for a wide range of empty states imaging conditions on the UO_2 (111) surface and implies that if there is any covalent coupling in stoichiometric UO_2 it is not easily detected by STM.

V. LSDA+U MODELING

As mentioned previously, the electronic structure of both NiO and UO_2 is affected fundamentally by the strong Coulomb correlations between electrons in the $3d$ shell of the Ni ions, and $5f$ shell of the U ions. In order to arrive at a model that accurately describes the band structure it is necessary to include the on-site electron repulsion term, involving the Hubbard U, in the *ab initio* calculation. The method used here is the LSDA+U approach, which is described in detail in Refs. 4 and 5.

A comparison of the calculated DOS of Ni $3d$ and O $2p$ orbitals using the LSDA+U method shows that there is significant hybridization between these orbitals,[5,8] resulting in a substantial degree of covalent bonding between Ni and O ions. The electron density distribution calculation for the (001) plane of bulk NiO is shown in Fig. 4. The Ni ions occupy the center and corner sites, and the O ions are situated on the center of the edges of the square. The map shows that the charge distribution around the O lattice positions is almost spherical, whereas the Ni ions display considerable anisotropy. This is a manifestation of covalent bonding effects in this oxide and also reflects the symmetry of Ni d orbitals forming electronic states near the Fermi energy. Careful examination the charge density map also reveals the tendency towards an antiferromagnetic tetragonal distortion of the cubic lattice of NiO which manifests itself through the top-right and bottom-left interatomic spaces having a lower charge density that the two other spaces.

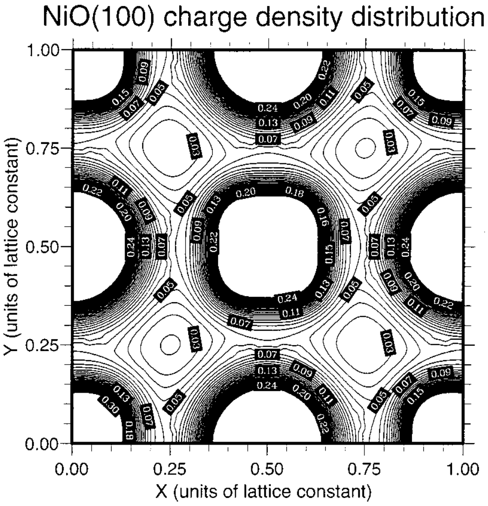

FIG. 4. Electron density map showing electron sharing between neighboring Ni and O ions in the bulk (100) plane.

While there is a covalent contribution to bonding in NiO, this cannot be observed in the equivalent LSDA+U charge density calculation for UO_2. Figure 5 shows a (110) plane through the charge density of bulk UO_2. A (110) plane is presented rather than a (111) plane because the (110) plane cuts through both oxygen and uranium ions whereas for the

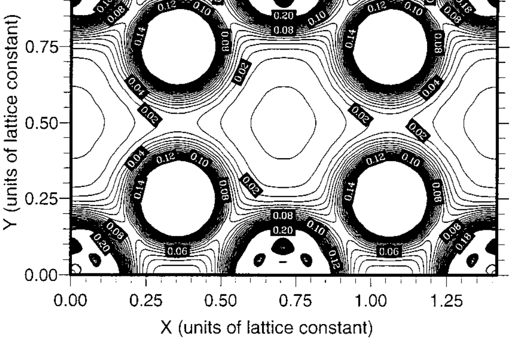

FIG. 5. Electron density map through the (110) plane of bulk UO_2. The charge density contours around both uranium and oxygen ions are spherical indicating that the bonding is predominantly ionic.

(111) plane one would have to choose whether to show only the uranium or oxygen sites. In Fig. 5 six uranium ions occupy the corner and long edge positions, and four oxygen ions are located towards the center of the plot. Unlike the Ni ions in NiO, the charge density around the U ions in Fig. 5 is almost spherical which can be treated as an indication that bonding in UO_2 is predominantly ionic. The distribution of charge around oxygen ions is spherical for both UO_2 and NiO.

VI. CONCLUSIONS

We have demonstrated that it is possible to obtain STM images at atomic resolution from surfaces of the room temperature insulators NiO and UO_2. This is achieved by imaging at elevated temperatures where the conductivity is sufficiently increased. By analyzing the STM results in combination with results from LSDA+U modeling, we have shown that there is a significant covalent contribution to bonding in NiO, but that UO_2 is predominantly ionic.

ACKNOWLEDGMENTS

We would like to thank Dr. W. P. Ellis for supplying and preparing the UO_2 crystal, and Dr. P. L. Wincott and Professor G. Thornton for involvement with the experimental work on NiO. We are grateful to Dr. S. Y. Savrasov for significant help with modeling. Financial support from British Nuclear Fuels plc (BNFL) and the EPSRC is gratefully acknowledged.

[1] V. E. Henrich and P. A. Cox, *The Surface Science of Metal Oxides* (Cambridge University Press, Cambridge, UK, 1994).
[2] V. I. Anisimov, J. Zaanen, and O. K. Andersen, Phys. Rev. B **44**, 943 (1991).
[3] A. I. Liechtenstein, V. I. Anisimov, and J. Zaanen, Phys. Rev. B **52**, R5467 (1995).
[4] S. L. Dudarev, D. Nguyen Manh, and A. P. Sutton, Philos. Mag. B **75**, 613 (1997).
[5] S. L. Dudarev, A. I. Liechtenstein, M. R. Castell, G. A. D. Briggs, and A. P. Sutton, Phys. Rev. B **56**, 4900 (1997).
[6] W. P. Ellis and R. L. Schwoebel, Surf. Sci. **11**, 82 (1968).
[7] M. R. Castell, P. L. Wincott, N. G. Condon, C. Muggelberg, G. Thornton, S. L. Dudarev, A. P. Sutton, and G. A. D. Briggs, Phys. Rev. B **55**, 7859 (1997).
[8] M. R. Castell, S. L. Dudarev, P. L. Wincott, N. G. Condon, C. Muggelberg, G. Thornton, D. Nguyen Manh, A. P. Sutton, and G. A. D. Briggs, Surf. Rev. Lett. **4**, 1003 (1997).
[9] M. R. Castell, C. Muggelberg, G. A. D. Briggs, and D. T. Goddard, J. Vac. Sci. Technol. B **14**, 966 (1996).
[10] C. Muggelberg, M. R. Castell, G. A. D. Briggs, and D. T. Goddard, Surf. Rev. Lett. (in press).
[11] W. P. Ellis, J. Chem. Phys. **48**, 5695 (1968).
[12] W. P. Ellis and T. N. Taylor, Surf. Sci. **75**, 279 (1978).
[13] W. P. Ellis and T. N. Taylor, Surf. Sci. **91**, 409 (1980).